GLUONIC STRUCTURE FROM INSTANTONS*

C. Weiss

Theory Center, Jefferson Lab, Newport News, VA 23606, USA

Received 27 February 2025, accepted 15 March 2025,
published online 16 April 2025

The instanton vacuum provides an effective description of chiral symmetry breaking by local topological fluctuations of the gauge fields, as observed in lattice QCD simulations. The resulting effective dynamics at momenta below $1/\bar{\rho} \approx 0.6$ GeV explains the basic features of light-quark correlation functions and is used extensively in studies of hadron structure. The instanton fields also make definite contributions to the gluonic structure of light hadrons, as expressed in the matrix elements of composite quark–gluon or gluon operators. The article reviews the gluonic structure of light hadrons (nucleon, pion) induced by instantons. This includes: *(i)* twist-2 parton distributions and momentum sum rule; *(ii)* twist-3 angular momentum and spin-orbit interactions; *(iii)* twist-3 and twist-4 quark–gluon correlations and power corrections; *(iv)* trace anomaly and hadron mass decomposition; *(v)* scalar gluon form factors and mechanical properties; *(vi)* axial anomaly and pseudoscalar gluon form factors. It also discusses possible further applications of the methods and recent developments including gauge field configurations beyond instantons.

DOI:10.5506/APhysPolB.56.3-A7

1. Introduction

Chiral symmetry breaking (ChSB) plays an essential role in the emergence of hadron structure from QCD. It is connected with the dynamical generation of mass in the world of light hadrons, including the baryons, and determines the effective dynamics governing their structure. It gives rise to nearly massless bosonic excitations, the pions, and restricts the form of their interactions with other hadrons. The long-distance behavior of strong interactions on the $1/M_\pi$ scale can be described by an effective field theory based on ChSB.

ChSB in QCD is caused by topological fluctuations of the gauge fields. In the sense of real-time evolution, these fields describe tunneling trajectories between configurations in sectors with different winding number [1–3]. The topological gauge fields induce zero-virtuality modes of the fermion field with definite chirality. ChSB arises from the delocalization of the zero modes at finite density of the topological gauge fields. The direct connection between ChSB and the zero modes is apparent from the Banks–Casher theorem, which states that the chiral condensate is proportional to the spectral density of the Dirac operator at zero virtuality [4].

The quantitative features of the topological gauge field fluctuations and ChSB in the imaginary-time (Euclidean) formulation have been investigated in lattice QCD. Cooling methods suppress quantum fluctuations and produce smooth configurations showing local concentrations of topological charge and action (see Fig. 1 for a visualization [5]); similar results are obtained with modern gradient flow techniques [6–8]. The typical size of the topological fluctuations is $\bar{\rho} \sim 0.3$ fm, much smaller than the hadronic size ~ 1 fm. The typical distance between the topological fluctuations is $\bar{R} \sim 1$ fm, and only a small fraction of 4-dimensional Euclidean space is occupied by such fields, $\pi^2\bar{\rho}^4/\bar{R}^4 \sim 0.1$. The average field strength inside the topological fluctuations is $(F_{\mu\nu}F_{\mu\nu})^{1/2} \sim (32\pi^2/\pi^2\bar{\rho}^4)^{1/2} \sim 2$ GeV^2, which is very large on the hadronic scale. Such strong fields present favorable conditions for a semiclassical description [1, 2].

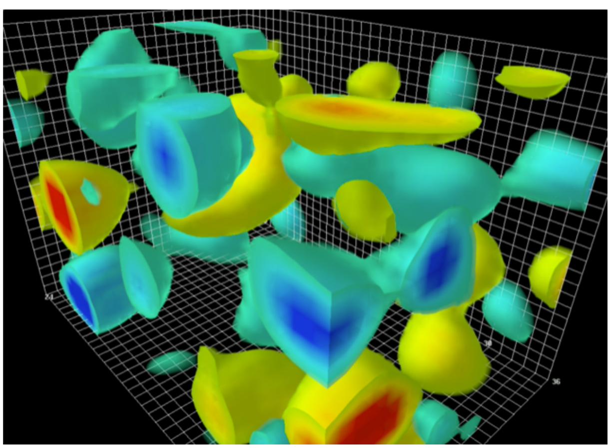

Fig. 1. Local concentrations of topological charge in cooled lattice configurations of gluodynamics [5]. Yellow: Positive charge (instantons). Blue: Negative charge (antiinstantons).

An effective description of ChSB by topological gauge fields is provided by the instanton vacuum [9, 10]; see Refs. [11, 12] for reviews. The basic idea is to separate the modes of the gauge fields according to the scale $\bar{\rho}^{-1}$ and perform the functional integration using different approximations (see Fig. 2). The modes with momenta $k < \bar{\rho}^{-1}$ are described as a superposition

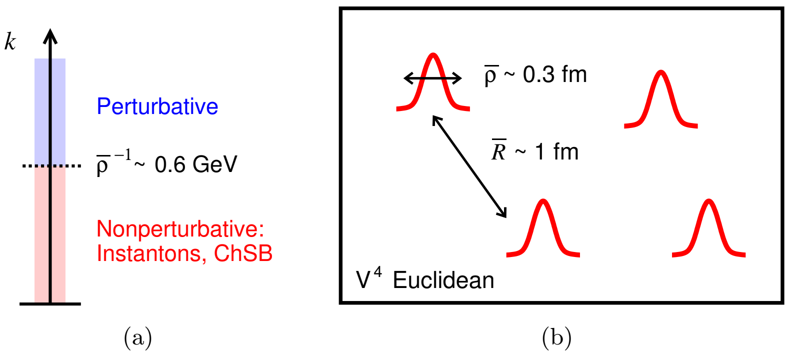

Fig. 2. Instanton vacuum. (a) Separation of modes according to the dynamical scale $\bar{\rho}^{-1}$. (b) Instanton ensemble describing the low-momentum modes.

of instantons and instantons-localized classical solutions with topological charge ± 1, and integrated using nonperturbative methods of statistical mechanics. The modes with $k > \bar{\rho}^{-1}$ are integrated perturbatively and enter in the statistical weight of the classical fields. The procedure can be formulated as a variational approximation to the QCD partition function [10]; questions such as the gauge dependence in the separation of modes, ansatz dependence in the superposition of instantons, *etc.*, are part of the "choice of trial function" and contained in the overall variational approximation. The construction uses the instanton packing fraction $\pi^2 \bar{\rho}^4/\bar{R}^4 \ll 1$ as a small parameter [9] and employs it in the functional integration. A stable ensemble is obtained by including instanton interactions derived from QCD [10]. The quantitative features agree well with those observed in lattice QCD. The picture is robust and does not depend on the details of the variational approximation [12].

ChSB in the instanton vacuum has been studied extensively and is well understood [13, 14]; see Refs. [11, 12] for reviews. The instantons induce multifermion interactions between the quarks through the fermion zero modes. The finite density of instantons in the vacuum leads to the formation of a chiral condensate, and the quarks acquire a dynamical mass $M \sim 0.3$–0.4 GeV, of the order of a typical constituent quark mass. The effective dynamics can be constructed and solved systematically in the $1/N_c$ expansion [14–19]. The interactions can be bosonized and take the form of massive quarks interacting with chiral meson fields. The resulting field theory captures the effective dynamics at Euclidean momenta $k < \bar{\rho}^{-1}$ and describes a wide range of structures and phenomena. Correlation functions in the meson sector exhibit the quasi-massless pion pole in the pseudoscalar–isovector channel and the massive η' pole in the isoscalar channel [15, 17, 19]; see Ref. [12] for a review of other channels. Correlation functions in the baryon sector are characterized by a localized classical chiral field ("soliton"), in which the quarks move in independent-particle orbits [20], providing a specific realization of the mean-field picture of baryons in the large-N_c limit of QCD [21]; see Ref. [22] for a review.

In the effective dynamics emerging from ChSB, the instanton gauge fields are subsumed in the massive quark/antiquark degrees of freedom. Hadronic matrix elements of QCD quark operators (vector or axial vector current, scalar density) can be obtained from the effective dynamics without explicit reference to instantons. The instanton vacuum also enables the computation of hadronic matrix elements of quark–gluon or pure gluon QCD operators, normalized at the scale $\bar{\rho}^{-1}$ [18, 19, 23]. In this context the instanton gauge fields appear explicitly and give rise to a definite "gluonic structure" of the light hadrons. Exploring this structure is interesting for several reasons:

(i) Gluon operators in the instanton vacuum are evaluated in an expansion in the instanton packing fraction. The small parameter enables a systematic analysis and establishes a hierarchy in the matrix elements of gluon operators with different quantum numbers (spin, twist).

(ii) The gluonic structure induced by instantons is derived using the same approximations as in the effective dynamics emerging from ChSB. This preserves the essential connections between the quark and gluon operators, *e.g.* the momentum sum rule for twist-2 operators, or QCD equation-of-motion relations for higher-twist operators.

(iii) The instanton fields are strong on the hadronic scale. In channels where single instantons are allowed to contribute, they likely represent the dominant effect in low-energy gluonic structure.

(iv) The gluon operators enable the direct demonstration of instanton effects in hadron structure. The selection rules implied by the symmetries of the instanton field are very distinctive and can be compared with observations.

(v) The instanton vacuum preserves the renormalization properties of QCD and implements the conformal (trace) anomaly through instanton density fluctuations. It enables study of the interplay of conformal and chiral symmetry breaking, which is essential for the mass decomposition of light hadrons. The instanton vacuum also implements the $\mathrm{U}(1)_{\mathrm{A}}$ axial anomaly through topological charge fluctuations and enables the study of its expression in hadron structure.

This article reviews the gluonic structure of light hadrons in the instanton vacuum. It covers the basic methods, established and recent results, and suggestions for future developments and applications. The treatment is based on the variational formulation of the instanton vacuum of Refs. [10, 14] and the effective operator method of Ref. [18], which permits systematic calculation and characterization of gluonic structure.

Section 2 introduces the elements of the instanton ensemble and ChSB needed in the present review. Section 3 describes the effective operator method for the study of gluonic structure. Section 4 reviews the main results in gluonic structure, organized according to the type of QCD operator; conclusions and suggestions for further studies are presented at the end of each subsection. Section 5 describes recent developments in extending the semiclassical approximation beyond instantons.

Theoretical models of the nonperturbative gluonic structure of the nucleon and other light hadrons are urgently needed for many problems of current interest, such as generalized parton distributions, the energy-momentum tensor (EMT) form factors and hadron mass decomposition (trace anomaly), higher-twist effects in inclusive and exclusive scattering, heavy-quark contributions to nucleon observables, heavy-quarkonium production at near-threshold energies, hadronic CP violation, and other phenomena. The instanton vacuum can classify and estimate the gluon matrix elements in a systematic fashion and make essential contributions to these areas of study.

The methods and results presented here are based on the renowned work of D.I. Diakonov and V.Yu. Petrov on the instanton vacuum, and represent only one of its many contributions to the understanding of nonperturbative QCD and hadron structure. The applications to gluonic structure reviewed here were in large parts developed by M.V. Polyakov and represent only a small part of his extensive and profound impact on modern hadronic physics. The effective operator method was proposed in a work by Diakonov, Polyakov, and this author as a junior collaborator. I had the fortune to work under the guidance of DPP and learn from them over an extended time and consider this the greatest blessing of my scientific and intellectual life. The best way in which our community can honor their memory is to move ahead with the same energy and enthusiasm, keep up the intellectual standards to the best of our abilities, realize the potential of the concepts and methods they developed, and pass them on to the next generation.

2. Effective dynamics from instantons

The basic elements of the instanton vacuum are described in Refs. [11, 12]. QCD is considered in 4-dimensional Euclidean space-time, with coordinates $x_\mu, \mu = 1$–4, and metric $x^2 \equiv \sum x_\mu^2 > 0$. The normalization volume V is finite and taken to be large, with densities such as N/V remaining stable in the limit.

2.1. Instanton ensemble

The conceptual framework is a variational approximation to the gluodynamics partition function [10] (see comments in Section 1). The low-momentum modes of the gauge potential ($k < \bar{\rho}^{-1}$) are parametrized by a sum of instanton and antiinstanton potentials in singular gauge (denoted by subscripts $\pm$)

$$A(x) = \sum_{I}^{N_+} A_+ (x|z_I, O_I, \rho_I) + \sum_{\bar{I}}^{N_-} A_- (x|z_{\bar{I}}, O_{\bar{I}}, \rho_{\bar{I}}) \; ; \tag{1}$$

the explicit form of $A_\pm$ is given in Refs. [11, 12]. Each instanton depends on a set of collective coordinates: the center coordinate z, color orientation O, and size ρ (see Fig. 3 (a)). The functional integration is performed as

$$\int \prod_{I,\bar{I}}^{N_\pm} \mathrm{d}z_I \, \mathrm{d}O_I \, \mathrm{d}\rho_I [\ldots] \, . \tag{2}$$

The high-momentum modes ($k > \bar{\rho}^{-1}$) are integrated out separately around each instanton, as justified *a posteriori* by the diluteness of the instanton medium, and result in a statistical weight per instanton [24]

$$d_0(\rho) = \text{const.} \times \rho^{-5} (\rho \Lambda_{\mathrm{QCD}})^b \times [\mathrm{NLO}] \, , \qquad b = \frac{11}{3} N_c - \frac{2}{3} N_f \, , \tag{3}$$

where b is the LO coefficient of the QCD beta function; see Refs. [12, 25] for details. The weight of Eq. (3) strongly increases at large sizes and would not in itself result in a stable system.

A stable system is obtained by including the effect of instanton interactions, which suppress instantons with a large size. This can be done consistently and efficiently with the variational approximation of Ref. [10]. The trial partition function is chosen as an ensemble of independent instantons with an effective size distribution

$$Z_{\mathrm{int}} = \int \prod_{I,\bar{I}}^{N_\pm} \mathrm{d}z_I \, \mathrm{d}O_I \, \mathrm{d}\rho_I \; d_{\mathrm{eff}}(\rho_I) \, . \tag{4}$$

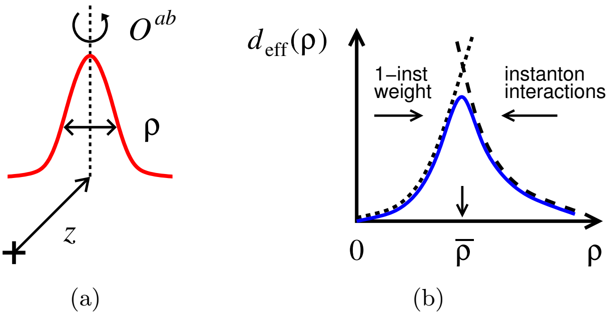

Fig. 3. (a) Collective coordinates characterizing the instanton. (b) Effective instanton size distribution of Eq. (5).

Performing a variational estimate of the full QCD partition function in terms of the trial partition function of Eq. (4), one can naturally identify the instanton interactions generated by QCD and evaluate their effect on the size distribution. The effective size distribution is obtained as

$$d_{\text{eff}}(\rho) = \text{const.} \times d_0(\rho)\, \mathrm{e}^{-\alpha\rho^2}\,, \qquad \alpha = \gamma \frac{8\pi^2}{g^2}\frac{N}{V}\,, \tag{5}$$

where γ is a constant characterizing the instanton interactions, g is the coupling constant at the scale $\bar{\rho}^{-1}$, and $N/V \equiv (N_+ + N_-)/V$ is the total instanton density. The distribution of Eq. (5) suppresses large sizes and leads to a stable system (see Fig. 3 (b)). In the large-N_c limit, the width of $d_{\text{eff}}(\rho)$ is $\mathcal{O}(1/N_c)$, so that fluctuations of the sizes are suppressed, and the averaging over sizes in the ensemble of Eq. (4) is performed by simply replacing $\rho \to \bar{\rho}$.

Numerical studies have been performed using various forms of the instanton interaction [10, 18]. The properties of the variational ensemble are not sensitive to the details of the interaction or other elements of the approximation. The average instanton size is obtained as $\bar{\rho} \sim 0.3$ fm, and the instanton packing fraction as

$$\kappa \equiv \pi^2 \bar{\rho}^4/\bar{R}^4 \sim 0.1\,, \tag{6}$$

consistent with the results of lattice simulations. The small value of the instanton packing fraction ("diluteness") justifies the approximations made in the functional integration and provides a small parameter for organizing the calculation of ensemble averages.

An important feature of the instanton ensemble is that all dynamical scales emerge from the QCD scale in the running coupling, Λ_{QCD}. No dimensionful parameters are introduced in the approximations; the instanton interactions are parametrized by dimensionless constants [10, 18]. As a consequence, all dynamical scales in the low-momentum sector ($k < \bar{\rho}^{-1}$), including the average size $\bar{\rho}$, can be expressed as powers of the instanton density N/V. In this way, the instanton density can be regarded as the fundamental scale in low-momentum dynamics, and all other scales arise from it through the nonlinearity of the dynamics [17–19]. This fact is essential for the realization of conformal symmetry breaking and the trace anomaly in the instanton vacuum (see Section 4.4).

2.2. Fermions and ChSB

When fermions are coupled to the instantons, the field of a single (anti-)instanton induces a zero-virtuality mode of the Dirac operator

$$\left[i\partial\!\!\!/_x + A_\pm(x|z,O,\rho)\right] \varPhi_\pm(x|z,O,\rho) = 0\,. \tag{7}$$

The zero-mode wave function $\varPhi_\pm$ is normalizable, localized at the position of the instanton, and depends on the collective coordinates of the instanton field. The zero mode has definite chirality, $\gamma_5\varPhi_\pm = \pm\varPhi_\pm$. The interaction of the fermion fields with the zero mode of a single instanton is described by the vertex created by the projector on the zero mode

$$V_\pm(z,O,\rho)\left[\psi^\dagger,\psi\right] \equiv \int \mathrm{d}^4 x' \psi^\dagger\left(x'\right) i\partial\!\!\!/ \varPhi_\pm\left(x'|\ldots\right) \int \mathrm{d}^4 x\, \varPhi^\dagger_\pm(x)\, i\partial\!\!\!/ \psi(x|\ldots)\,, \tag{8}$$

where $\psi^\dagger \equiv i\bar{\psi}$. In the presence of $N_f \geq 1$ light flavors, the instanton interacts with all of them (see Fig. 4 (a)). By averaging over the color orientation of the instanton, one obtains a vertex of the form

$$\int \mathrm{d}O \prod_f^{N_f} V_\pm(z,O,\rho)\left[\psi^\dagger_f,\psi_f\right] = \text{const.} \times \det \psi^\dagger(z)\,\overleftarrow{F}\gamma_\pm\overrightarrow{F}\,\psi(z)\,, \tag{9}$$

where $\gamma_\pm \equiv (1 \pm \gamma_5)/2$ is the chiral projector. The vertex has the characteristic form of the determinant of the $N_f \times N_f$ matrix formed by the flavor components of the quark fields and involves all light flavors in the system ('t Hooft vertex, see Fig. 4 (b)) [24]. From Eq. (9),

$$\overrightarrow{F}\psi(z) \equiv \int \frac{\mathrm{d}^4 p}{(2\pi)^4}\, \mathrm{e}^{ip\cdot z} F(p)\psi(p)\,, \tag{10}$$

$$\psi^\dagger(z)\overleftarrow{F} \equiv \int \frac{\mathrm{d}^4 p'}{(2\pi)^4}\, \mathrm{e}^{-ip'\cdot z} \psi^\dagger\left(p'\right) F\left(p'\right)\,, \tag{11}$$

where $F(p)$ is a form factor arising from the wave function of the zero mode in momentum representation, with $F(0) = 1$, and $F(p) \to 0$ for $p > \rho^{-1}$ [18]. The vertex thus has a finite range, given by the instanton size ρ.

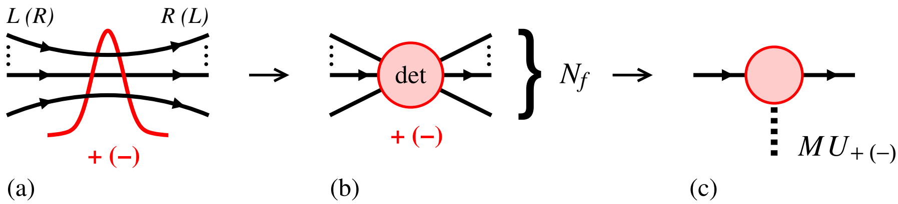

Fig. 4. Fermion interactions induced by instantons. (a) Fermions in the (anti-) instanton field (L, R denote the chirality). (b) Flavor interaction from averaging over the color orientation ('t Hooft vertex). (c) Interaction with the chiral field from bosonization.

In the ensemble with a finite density of instantons, the fermion zero modes cause ChSB. The phenomenon can be understood as the delocalization of the zero modes created by the individual instantons and is analogous to band formation in the electron structure of solids [11, 12]. It can be demonstrated by studying the propagation of fermions in the multiinstanton background using the Green function [14, 16] or effective action methods [15, 18, 19]. In the large-N_c limit, the functional integral over the fermions can be computed in the saddle-point approximation. A nontrivial saddle point appears, characterized by a dynamical quark mass M of parametric order $M^2 \sim \kappa\bar{\rho}^{-2}$, with a numerical value of $M \sim$ 0.3–0.4 GeV.

The functional integral can be bosonized by introducing meson fields $\mathcal{M}_\pm(x)$, which are $N_f \times N_f$ matrices in flavor. At the saddle point,

$$\mathcal{M}_\pm(x)_{f'f} \propto \left\langle \mathrm{det}'_{f'f}\, \psi^\dagger(x)\overleftarrow{F}\gamma_\pm\overrightarrow{F}\psi(x)\right\rangle , \tag{12}$$

where $\langle \dots \rangle$ denotes the average over the fermion fields and $\mathrm{det}'_{f'f}$ is the minor of the flavor determinant with row f and column f' removed. This makes it possible to convert the multifermion interaction at the saddle point to an interaction of the quarks with the meson field

$$\det \psi^\dagger(x)\overleftarrow{F}\gamma_\pm\overrightarrow{F}\psi(x) \;\; \rightarrow \;\; \psi^\dagger(x)\overleftarrow{F}\gamma_\pm\mathcal{M}_\pm(x)\overrightarrow{F}\psi(x)\,. \tag{13}$$

In many applications, the meson field can be restricted to the chiral degrees of freedom and is parametrized as

$$\mathcal{M}_\pm(x) = MU_\pm(x)\,, \qquad U_\pm(x) = \mathrm{e}^{\pm i\pi^a(x)\tau^a}\,, \tag{14}$$

where $U_\pm$ are SU(N_f) unitary unimodular matrices, π^a is the pion field, and τ^a are the generators of the SU(N_f) algebra. At the saddle point, the effective action of the fermions can then be represented as [14, 15, 18, 19]

$$S_{\text{eff}}(x) = \int \mathrm{d}^4 x \, \psi^\dagger(x) \left[-i\partial\!\!\!/ - iM \overleftarrow{F} U^{\gamma_5}(x) \overrightarrow{F} \right] \psi(x) \,, \tag{15}$$

$$U^{\gamma_5}(x) \equiv \gamma_+ U_+(x) + \gamma_- U_-(x) = \mathrm{e}^{i\gamma_5 \pi^a(x) \tau^a} \,. \tag{16}$$

It describes the coupling of the massive quarks to the chiral meson field and captures the low-energy dynamics emerging from ChSB ($k < \bar{\rho}^{-1}$). The form of the coupling is dictated by chiral invariance and can be derived from general considerations [26]. The instanton vacuum provides the dynamical mechanism of ChSB, predicts the value of the dynamical quark mass, and defines the range of the effective interaction.

Hadronic correlation functions in the effective theory can be computed in the $1/N_c$ expansion. Meson correlation functions exhibit the quasi-massless pion pole in the pseudoscalar–isovector channel, and the massive η' pole in the isoscalar channel [in this channel the pseudoscalar U_1 degrees of freedom in the meson field Eq. (12) must be retained] [14, 15, 19]. Baryon correlation functions are characterized by a classical chiral field ("soliton"), in which the quarks move in independent-particle orbits [20]. The calculation of nucleon matrix elements of quark operators (vector/axial currents, scalars) in this approach has been discussed extensively in the literature; see Ref. [22] for a review.

Instantons convert the QCD color interactions at low energies to effective spin-flavor interactions. This effect plays an essential role in the emergence of hadron structure from QCD. The same effect is observed in the gluonic structure of light hadrons induced by instantons in Section 3.

The effective spin-flavor interactions induced by instantons have specific quantum numbers as encoded in the 't Hooft vertex Eq. (9). The interactions occur in the scalar/pseudoscalar channel and have the characteristic determinantal flavor dependence. The instanton-induced interactions give rise to ChSB, but this effect is not unique to the specific quantum numbers and could also be obtained from other effective interactions. The instanton-induced interactions also give rise to other effects which attest to the specific spin-flavor quantum numbers, such as the η' mass, the differences between vector and scalar correlation functions, and others [12]. The expression of instantons in low-energy dynamics thus extends beyond ChSB and can be observed in specific spin-flavor-dependent phenomena.

3. Effective operators from instantons

The instanton vacuum allows one to compute correlation functions of QCD operators involving the gauge fields. Such operators can be converted to "effective operators" in the effective theory of massive quarks with chiral interactions emerging after ChSB [18]. The effective operators provide a concise representation of the instanton effects in the QCD operators and enable efficient computation of the hadronic matrix elements.

Consider a gauge-invariant composite QCD operator involving the gauge potential, $\mathcal{O}[A, \psi^\dagger, \psi]$, normalized at the $\mu = \bar{\rho}^{-1}$ scale. In the scheme of approximations based on the separation of modes (see Fig. 2 (a)), the gauge potential in the operator is identified with the classical field of the superposition of instantons, Eq. (1). In leading order of the packing fraction, the function of the gauge potential can be approximated by the sum of the functions evaluated in the fields of the individual instantons

$$\mathcal{O}\left[A, \psi^\dagger, \psi\right] \to \sum_{I+\bar{I}} \mathcal{O}\left[A_I, \psi^\dagger, \psi\right] . \tag{17}$$

The integration over the collective coordinates of the active instanton, combined with the coupling of the instanton to the fermions through the zero mode, converts the gluon operator into an effective fermion operator. The effective operator is defined such that

$$\left\langle \ldots\, \mathcal{O}\left[A, \psi^\dagger, \psi\right] \ldots \right\rangle_{\text{inst}} \stackrel{!}{=} \left\langle \ldots\, \mathcal{O}_{\text{eff}}\left[\psi^\dagger, \psi\right] \ldots \right\rangle_{\text{eff}} , \tag{18}$$

i.e., the correlation functions of the effective operator in the effective theory of massive quarks ("after" integration over instantons) reproduce the correlation functions of the original quark–gluon operator in the instanton ensemble with quarks ("before" integration over instantons). The expression of the effective operator is derived in the saddle-point approximation, going through the same steps as in deriving the effective action. It is given by [18]

$$\begin{aligned} \mathcal{O}_{\text{eff}}\left[\psi^\dagger, \psi\right] \;=\; & \mathcal{N} \sum_{\pm} \int \mathrm{d}z\, \mathrm{d}O\, \mathrm{d}\rho\, d_{\text{eff}}(\rho) \\ & \times \mathcal{O}\left[A_\pm(z, O, \rho), \psi^\dagger, \psi\right] \prod_f^{N_f} V_\pm(z, O, \rho)\left[\psi_f^\dagger, \psi_f\right] , \end{aligned} \tag{19}$$

where $A_\pm$ is the gauge potential of the single instanton coupling to the operator and $V_\pm$ is its zero mode vertex of Eq. (8). Both depend on the collective coordinates of the instanton, and the integration connects the

QCD operator with the instanton-induced interactions. The normalization factor $\mathcal{N}$ is determined within the saddle-point approximation and discussed in Refs. [18, 27].

The form of the effective operator depends on the color structure of the QCD operator. One class of QCD operators has the structure

$$\mathcal{O}\left[A, \psi^\dagger, \psi\right] = \psi^\dagger(x) \varGamma \psi(x) \mathcal{F}[A] \,, \tag{20}$$

where the quark bilinear is a color-singlet and $\mathcal{F}[A]$ is a color-singlet function of the gauge fields (both $\varGamma$ and $\mathcal{F}$ may carry Lorentz indices, which are omitted for brevity). In this case, the operator in the instanton field does not depend on the instanton color orientation, and

$$\mathcal{F}\left[A_\pm(z, O, \rho)\right] = \mathcal{F}_\pm(x - z|\rho) \,, \tag{21}$$

where $\mathcal{F}_\pm$ is a scalar function of the coordinates and the size ρ. The color average in Eq. (19) is then the same as in the fermion vertex of Eq. (9), and the gluon part of the operator becomes the 't Hooft vertex

$$\begin{aligned} \mathcal{O}_{\text{eff}}\left[\psi^\dagger, \psi\right] &= \psi^\dagger(x) \varGamma \psi(x) \times \mathcal{N} \sum_\pm \int \mathrm{d}^4 z \; \mathcal{F}_\pm(x - z|\bar\rho) \\ &\quad \times \det \psi^\dagger(z) \overleftarrow{F} \gamma_\pm \overrightarrow{F} \psi(z) \,. \end{aligned} \tag{22}$$

A similar form applies to pure gluon QCD operators without the quark bilinear, $\mathcal{O}[A] = \mathcal{F}[A]$ [28].

Another class of QCD operators has the structure

$$\mathcal{O}\left[A, \psi^\dagger, \psi\right] = \psi^\dagger(x) \varGamma \frac{\lambda^a}{2} \psi(x) \; \mathcal{F}^a[A](x) \,, \tag{23}$$

where the quark bilinear is the color-octet current of the quark field and $\mathcal{F}^a[A]$ is a color-octet function of the gauge potential (see Fig. 5 (a)). In the field of the instanton, the color-octet function takes the form (see Fig. 5 (b))

$$\mathcal{F}^a\left[A_\pm(z, O, \rho)\right](x) = O^{ab} \eta^b_{\mp\mu\nu} \mathcal{F}_{\pm\mu\nu}(x - z|\rho) \,, \tag{24}$$

where $\eta_{\mp\mu\nu} \equiv \bar\eta_{\mu\nu}, \eta_{\mu\nu}$ are the 't Hooft symbols and $\mathcal{F}_{\pm\mu\nu}$ is a tensor-valued function of the coordinates and the size ρ. In this case the function of the instanton field depends on the color orientation, and the average in Eq. (19) entangles the function with the zero-mode projector. The effective operator now becomes (see Fig. 5 (c))

$$\mathcal{O}_{\text{eff}}\left[\psi^\dagger,\psi\right] = \psi^\dagger(x)\Gamma\frac{\lambda^a}{2}\psi(x)\times\mathcal{N}\sum_{\pm}\int d^4z\,\mathcal{F}_{\pm\mu\nu}(x-z|\bar{\rho})$$
$$\times\sum_{ff'}\psi^\dagger{}_{f'}(z)\overleftarrow{F}\frac{\lambda^a}{2}\sigma_{\mu\nu}\gamma_\pm\overrightarrow{F}\psi_f(z)\,\det{}'_{f'f}\,\psi^\dagger(z)\overleftarrow{F}\gamma_\pm\overrightarrow{F}\psi(z)\,. \tag{25}$$

The flavor determinant gets "differentiated", and one of the quark bilinears is now the color-octet Lorentz-tensor projection of the quark fields.

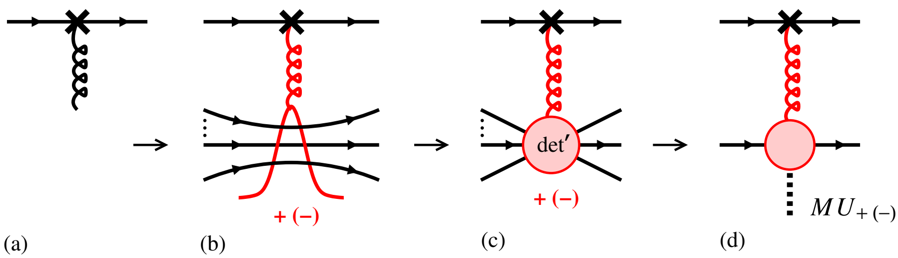

Fig. 5. Effective operators from instantons [here for a color-octet QCD operator of the form of Eq. (23)]. (a) QCD quark–gluon operator. (b) Operator with the gluon field evaluated in an (anti-) instanton. (c) Effective fermion operator from averaging over the collective coordinates. (d) Bosonized form of the effective operator.

The effective operators induced by instantons are originally obtained as multifermion operators, Eqs. (22) and (25). When used in correlation functions in the bosonized effective theory of Eq. (15), the multifermion effective operators can be converted to the bosonized form, applying the same techniques as in the bosonization of the effective action, see Eq. (12). The bosonized form of the color-octet effective operator of Eq. (25) is (see Fig. 5 (d))

$$\mathcal{O}_{\text{eff}}\left[\psi^\dagger,\psi\right] = \psi^\dagger(x)\Gamma\frac{\lambda^a}{2}\psi(x)\times\frac{iM}{N_c}\sum_{\pm}\int d^4z\,\mathcal{F}_{\pm\mu\nu}(x-z|\bar{\rho})$$
$$\times\psi^\dagger(z)\overleftarrow{F}\frac{\lambda^a}{2}\sigma_{\mu\nu}U_\pm(z)\gamma_\pm\overrightarrow{F}\psi(z)\,. \tag{26}$$

Here, the coefficient is given by dynamical quark mass M; its value is unambiguously determined within the scheme of approximations. This shows the close connection between the effective dynamics and the effective operators in the instanton vacuum.

Hadronic matrix elements are computed by inserting the effective operators in correlation functions and evaluating them using the same methods as for quark operators ($1/N_c$ expansion); see Refs. [27, 29] for an overview.

The effective operators illustrate the conversion of color interactions to spin-flavor interactions by the instantons, as already observed in the effective dynamics (see Section 2). The different color structure of the QCD operators of Eqs. (20) and (23), gives rise to a different spin-flavor structure of the effective operators, see Eqs. (22) and (25). It implies a spin-flavor dependence of the gluonic structure of hadrons, as can be seen in the hadronic matrix elements.

The expressions of Eqs. (19) and the following apply to the effective operators in leading order of the packing fraction, where the gauge field in the QCD operator is that of a single instanton. Recent work has derived the effective operators including also instanton–antiinstanton pairs, which give rise to additional spin-flavor structures (see Section 5) [23, 30].

4. Gluonic structure from instantons

4.1. Twist-2 parton distributions and momentum sum rule

The effective operator method can be used to evaluate hadronic matrix elements of various QCD quark–gluon and pure gluon operators in the instanton vacuum. It is helpful to organize the discussion according to the twist (= mass dimension minus spin) of the operators, as this property is important for the size of the instanton effects and the parametric order of the effective operators. In the following, the QCD operators and the instanton-induced effective operators are presented in the Minkowskian form (4-vectors, fields, gamma matrices) to facilitate comparison with phenomenology; see Refs. [12, 29] for the Euclidean–Minkowskian correspondence.

Twist-2 QCD operators describe scaling contributions to the DIS structure functions. The twist-2 quark and gluon operators of spin-2 are the rank-2 symmetric traceless tensors

$$
\begin{aligned}
\mathcal{O}_f^{\alpha\beta}(x) &\equiv \frac{1}{2}\bar{\psi}_f(x)\gamma^{\{\alpha}i\nabla^{\beta\}}\,\psi_f(x) - \text{trace} \\
&= \frac{1}{2}\bar{\psi}_f(x)\gamma^{\{\alpha}\left(i\partial^{\beta\}} + \frac{\lambda^a}{2}\,(A^a)^{\beta\}}\,(x)\right)\psi_f(x) - \text{trace}\,, \qquad (27)
\end{aligned}
$$

$$
\mathcal{O}_g^{\alpha\beta}(x) \equiv F_\gamma^{\ \{\alpha}(x)F^{\beta\}\gamma}(x) - \text{trace}\,, \qquad (28)
$$

where $\{\alpha\beta\} \equiv \alpha\beta + \beta\alpha$. The effective operators can be determined using the methods summarized in Section 3. The gluon part of the twist-2 quark operator of Eq. (27) is of the color-octet form operator of Eq. (23), and the effective operator is given by the general formula of Eq. (25). The explicit calculation shows that, when the multifermion effective operator is inserted in correlation functions and the quark fields are contracted, the result is of the order of $M^2\bar{\rho}^2 \sim \kappa$ and thus suppressed in the packing fraction of Eq. (6) [27, 31]. The twist-2 gluon operator of Eq. (28) is zero in the field of one instanton, and its effective operator is zero in leading order of the packing fraction. Altogether, the twist-2 effective operators are obtained as

$$\left(\mathcal{O}_f^{\alpha\beta}\right)_{\text{eff}}(x) = \frac{1}{2}\bar{\psi}_f(x)\gamma^{\{\alpha}\partial^{\beta\}}\psi_f(x) - \text{trace} + \mathcal{O}(\kappa)\,, \tag{29}$$

$$\left(\mathcal{O}_g^{\alpha\beta}\right)_{\text{eff}}(x) = \qquad 0 \qquad + \mathcal{O}(\kappa)\,. \tag{30}$$

The twist-2 quark operators are $\mathcal{O}(1)$ in the instanton packing fraction. The effect of the gauge potential in the covariant derivative of the QCD operators is suppressed, and the effective operator is given by the twist-2 operator in the massive quark fields formed with ordinary derivatives. The twist-2 gluon operator is $\mathcal{O}(\kappa)$ and suppressed in the packing fraction. These conclusions follow from the symmetry properties of the gauge potential/field of a single instanton, in particular its $O(4)$ rotational covariance [27, 31].

The spin-2 twist-2 operators constitute the spin-2 part of the QCD EMT. Their forward matrix elements (zero momentum transfer) in the nucleon or pion state define the light-cone momentum fraction carried by quarks/antiquarks and gluons in the hadron

$$\langle p|\textstyle\sum_f \mathcal{O}_f^{\alpha\beta}(0)\,|p\rangle \;=\; 2A_q\left(p^\alpha p^\beta - \text{trace}\right)\,, \tag{31}$$

$$\langle p|\mathcal{O}_g^{\alpha\beta}(0)\,|p\rangle \;=\; 2A_g\left(p^\alpha p^\beta - \text{trace}\right)\,. \tag{32}$$

The effective operators of Eqs. (29) and (30) imply that

$$A_q = 1 + \mathcal{O}(\kappa)\,, \qquad A_g = \mathcal{O}(\kappa)\,, \tag{33}$$

so that the light-cone momentum sum rule is satisfied in leading order of the packing fraction

$$A_q + A_g = 1 + \mathcal{O}(\kappa)\,. \tag{34}$$

This is a crucial test of the consistency of the approximations. In the instanton vacuum, the momentum sum rule is saturated by quarks and antiquarks in leading order of the packing fraction, and gluons are suppressed.

These findings can be generalized to the quark and gluon twist-2 operators of spin $n > 2$

$$\mathcal{O}_f^{\alpha_1\ldots\alpha_n} \;=\; \bar{\psi}_f(x)\gamma^{\{\alpha_1}\nabla^{\alpha_2}\ldots\nabla^{\alpha_n\}}\psi_f(x) - \text{traces}\,, \tag{35}$$

$$\mathcal{O}_g^{\alpha_1\ldots\alpha_n} \;=\; F_\gamma{}^{\{\alpha_1}D^{\alpha_2}\ldots D^{\alpha_{n-1}}F^{\alpha_n\}\gamma} - \text{traces}\,. \tag{36}$$

In leading order of the packing fraction, the twist-2 spin-n quark operator is given by the rank-n symmetric tensor operator in the ordinary derivatives of the massive quark field; the effect of the gauge potential in the covariant derivatives is suppressed. The twist-2 spin-n gluon operator is zero in the field of a single instanton.

The nucleon matrix elements of the twist-2 QCD operators define the moments of the nucleon parton distributions. The effective theory derived from the instanton vacuum can be used to compute the nucleon parton distributions directly as functions of the light-cone momentum fraction x. Calculations have been performed by evaluating the effective light-cone operators in a nucleon state at rest [32], and by using the equivalent formulation in terms of particle densities in a state with the large 3-momentum $p \to \infty$ [33]. In this picture, the nucleon's partonic structure is carried by the quark and antiquark distributions; the gluon distribution is suppressed. The antiquark distribution is $\mathcal{O}(1)$ and exhibits a rich spin and flavor dependence, generated by the classical chiral field. In particular, the picture predicted a large polarized antiquark flavor asymmetry $\Delta\bar{u}(x) - \Delta\bar{d}(x)$, which appears in leading order of the $1/N_c$ expansion [32, 33]. The prediction agrees with results of experiments in W^+ production in polarized pp collisions at RHIC [34–37] and a global analysis of the polarized sea-quark distributions [38]. It can also be tested with lattice QCD calculations using quasi/pseudo-distribution method [39].

In summary, at the level of twist-2 structure, and in leading order of the instanton packing fraction, the instanton fields are "subsumed" in the interactions in the effective theory and not manifest in partonic content. The partonic content is given by quarks and antiquarks. ChSB determines the effective interactions that create the quark/antiquark distributions and their spin and flavor dependence. The dynamical mass of the quarks/antiquarks is not manifest directly in the parton distributions; it is a part of the interactions in the system that define the parton distributions, not an elementary property of the particles being measured by the partonic operators. This picture is specific to twist-2 structure and is qualitatively different in higher-twist structure (see Section 4.2 and following).

Recent developments enable computation of the twist-2 quark and gluon densities at next-to-leading order of the packing fraction, including effects of instanton–antiinstanton molecules (see Section 5) [23, 40, 41]. Results for the momentum fractions A_q and A_g in the pion show numerically small $\mathcal{O}(\kappa)$ contributions [42]. Explaining the nucleon's twist-2 gluon density remains a prime task. Fits to DIS data with valence-like input densities at low scales of $\mu \gtrsim 0.5$ GeV [43] give large gluon momentum fractions $A_g \sim 0.3$–0.4, showing the need for sizable contributions from mechanisms other than single instantons.

4.2. Twist-3 angular momentum and spin-orbit interactions

Twist-3 QCD operators appear in the decomposition of the QCD angular momentum in spin and orbital contributions, and in the description of quark spin-orbit correlations in the nucleon. The nonforward matrix elements of these operators receive $\mathcal{O}(1)$ contributions from instantons and represent a unique case of gluonic structure induced by instantons [31].

The twist-3 QCD operator with natural parity is given by the antisymmetric rank-2 tensor

$$\begin{aligned}\mathcal{O}^{\alpha\beta}(x) &\equiv \frac{1}{2}\bar{\psi}(x)\gamma^{[\alpha} i \overleftrightarrow{\nabla}^{\beta]}\, \tau\, \psi(x) \\ &= \frac{1}{2}\bar{\psi}(x)\gamma^{[\alpha}\left(i\overleftrightarrow{\partial}^{\beta]} + \frac{\lambda^a}{2}(A^a)^{\beta]}(x)\right)\tau\,\psi(x)\,, \end{aligned} \tag{37}$$

where $\overleftrightarrow{\partial} = \frac{1}{2}(\overrightarrow{\partial} - \overleftarrow{\partial})$ and $[\alpha\beta] \equiv \alpha\beta - \beta\alpha$. τ denotes a flavor matrix and can be a singlet ($\tau = 1$) or non-singlet ($\tau = \tau^a$, $a = 1, 2, 3$ for $N_f = 2$). The operator of Eq. (37) with the flavor-singlet matrix represents the antisymmetric part of the QCD EMT [the symmetric part is given by Eq. (27)], and its nonforward matrix elements describe the spatial distribution of quark spin in hadrons [44].

The QCD operator of Eq. (37) contains the gauge potential in the covariant derivative. The gauge-potential-dependent term is of the form of Eq. (23), and the effective operator in the instanton vacuum is given by Eq. (26), where the function $\mathcal{F}_{\pm\mu\nu}$ now is the instanton gauge potential [31]. Equation (26) represents the effective operator as a four-fermion operator, formed by the product of two color-octet in the background of the chiral field (see Fig. 5 (d)). When inserted in hadronic correlation functions, the fields in the color-octet currents in the operator are contracted, reducing the operator to a two-fermion operator (see Fig. 6 (a)). The loop integral resulting from the contraction can be computed and is parametrically large $\sim \bar{\rho}^{-2}$ (it would be quadratically divergent for pointlike vertices and is rendered finite by zero mode form factors). The integral $\sim \bar{\rho}^{-2}$ compensates a factor $\sim \bar{\rho}^2$ contained in the function $\mathcal{F}_{\pm\mu\nu}$ and gives a result that is independent of the instanton size (see Fig. 6 (b)). Altogether, the effective operator for the twist-3 QCD operator of Eq. (37) is obtained as [31]

$$\left(\mathcal{O}^{\alpha\beta}\right)_{\rm eff}(x) = \frac{1}{2}\bar{\psi}(x)\left(\gamma^{[\alpha} i\overleftrightarrow{\partial}^{\beta]}\tau + \frac{iM}{2}\sigma^{\alpha\beta}[\tau, U^{\gamma_5}(x)]\right)\psi(x)\,. \tag{38}$$

The first term results from the quark field derivatives in the QCD operator of Eq. (37). The second term results from the gauge potential in the QCD operator through the instanton. The instanton converts the color interaction in the QCD operator to a spin-flavor interaction of the quark with the chiral field in the effective operator, with a coefficient given by the dynamical quark mass. (Here, the effective operator is presented for energies/momenta $p \sim M \ll \bar{\rho}^{-1}$, for which the zero-mode form factors in the external quark momenta can be neglected, $F \to 1$.)

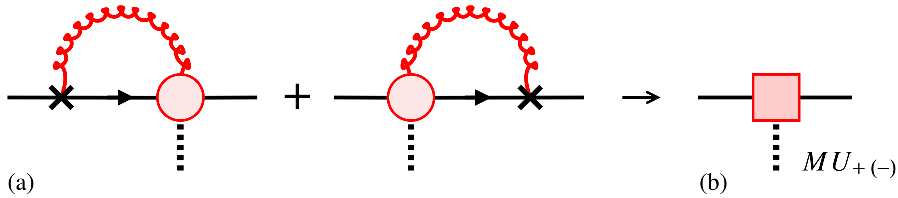

Fig. 6. (a) Contraction of the bosonized effective operator (see Fig. 5 (d)). (b) Resulting chiral quark operator. The dashed lines denote the chiral meson field.

The twist-3 QCD operator Eq. (37) satisfies an operator relation due to the QCD equations of motion. Using the QCD equations of motion for the quark fields,

$$\overrightarrow{\nabla\!\!\!/}\,\psi(x) = 0\,, \qquad \bar{\psi}(x)\overleftarrow{\nabla\!\!\!/} = 0\,, \tag{39}$$

the QCD operator of Eq. (37) can equivalently be expressed as the total derivative of the QCD axial vector current

$$\mathcal{O}^{\alpha\beta}(x) = -\frac{1}{4}\epsilon^{\alpha\beta\gamma\delta}\partial_\gamma\left[\bar{\psi}(x)\gamma_\delta\gamma_5\tau\psi(x)\right]\,, \tag{40}$$

where $\partial_\gamma[\ldots]$ denotes the total derivative. The effective operator of Eq. (38) satisfies the same relation in the effective theory of massive quarks with chiral interactions [31]. Using the equations of motion of the quark fields in the effective theory (here in the Minkowskian convention)

$$\left[i\overrightarrow{\partial\!\!\!/} - MU^{\gamma_5}(x)\right]\psi(x) = 0\,, \qquad \bar{\psi}(x)\left[-i\overleftarrow{\partial\!\!\!/} - MU^{\gamma_5}(x)\right] = 0\,, \tag{41}$$

the effective operator of Eq. (38) can be converted to the total derivative of the axial current in the effective theory

$$\left(\mathcal{O}^{\alpha\beta}\right)_{\text{eff}}(x) = -\frac{1}{4}\epsilon^{\alpha\beta\gamma\delta}\partial_\gamma\left[\bar{\psi}(x)\gamma_\delta\gamma_5\tau\psi(x)\right]_{\text{eff}}\,. \tag{42}$$

This remarkable result is obtained thanks to the chiral interaction term in the effective operator induced by instantons. It attests to the consistency of the approximations in the derivation of the effective action and the effective operator (packing fraction expansion, $1/N_c$ expansion). The QCD equation of motion in the effective operator is realized because the single instanton is a solution to the Yang–Mills equation. Similar equation-of-motion relations have been demonstrated for other higher-twist operators in the instanton vacuum [27]. An important consequence is that the results of the effective operator calculations are the same for different QCD operators related by QCD equations of motion and thus do not depend on the choice of operator basis used for the QCD operator analysis.

The matrix element of the twist-3 QCD operator of Eq. (37) describes the spatial distribution of quark spin in the nucleon [44]. The effective operator of Eq. (38) reveals an interesting flavor dependence. The instanton-induced interaction term in Eq. (38) is proportional to the flavor commutator $[\tau, U^{\gamma_5}(x)]$. In the flavor-singlet operator ($\tau = 1$), the interaction term is zero. The total spin distribution is thus not affected by the instanton-induced interactions. This is consistent with the fact that the total spin distribution can be derived from the EMT in the effective theory, obtained as the conserved current associated with the space-time symmetries. In the flavor-nonsinglet operator ($\tau = \tau^3$ for $N_f = 2$), the interaction effect is nonzero. The spin distributions of individual quark flavors are, therefore, affected by the instanton-induced interactions.

The twist-3 QCD operator analogous to Eq. (37) with unnatural parity,

$$\mathcal{O}_5^{\alpha\beta}(x) \equiv \frac{1}{2}\bar{\psi}(x)\gamma^{[\alpha}\gamma_5 i\overleftrightarrow{\nabla}^{\beta]}\,\tau\,\psi(x)\,, \tag{43}$$

describes the spin-orbit correlations of quarks in QCD [45]. Its effective operator has been derived, going through the same steps as for the natural parity operator, and is given by [31]

$$\left(\mathcal{O}_5^{\alpha\beta}\right)_{\text{eff}}(x) = \frac{1}{2}\bar{\psi}(x)\left(\gamma^{[\alpha}\gamma_5 i\overleftrightarrow{\partial}^{\beta]}\tau + \frac{iM}{2}\sigma^{\alpha\beta}\gamma_5\{\tau, U^{\gamma_5}(x)\}\right)\psi(x)\,. \tag{44}$$

It exhibits a similar instanton-induced interaction term as the natural-parity operator of Eq. (38) and satisfies similar equation-of-motion relations. In the unnatural-parity operator of Eq. (44), the interaction term is now proportional to the flavor anticommutator $\{\tau, U^{\gamma_5}(x)\}$, and is, therefore, nonzero also in the flavor-singlet operator. The interaction term plays an essential role in the theory of spin-orbit correlation of quarks in the nucleon (see Fig. 7). Its mechanical interpretation in the mean-field picture of the nucleon in large-N_c limit has been explored in Ref. [46].

The twist-3 operators of Eqs. (37) and (43) have hadronic matrix elements proportional to the momentum transfer p'–p between the states, which vanish in the forward limit. This can be seen from the fact that the operators can be converted to total derivative operators using the equations of motion. Large instanton effects in thetwist-3 operators have so far only

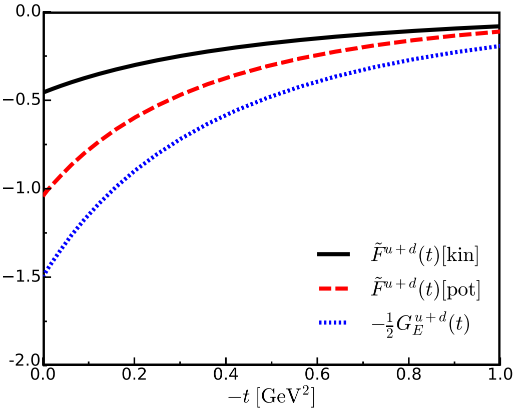

Fig. 7. Nucleon form factor $\tilde{F}^{u+d}(t)$ of the twist-3 QCD operator of Eq. (43) obtained from the instanton vacuum [46]. Black solid line: Contribution of quark field derivative in effective operator of Eq. (44). Dashed red line: Contribution of chiral interaction term induced by instantons in effective operator of Eq. (44). Dotted blue line: Total result, satisfying the sum rule $\tilde{F}^{u+d}(t) = -\frac{1}{2}G_E^{u+d}(t)$ (nucleon vector form factor).

been observed in the “nonforward” operators presented here; in other twist-3 operators, the effects of the instanton field are suppressed (see Section 4.3).

In summary, in the twist-3 QCD operators, the instanton field can cause O(1) effects, by converting the color interaction in the QCD operator into a chiral spin-flavor interaction in the effective operator. This dynamical effect has important consequences for the flavor dependence of the quark spin distributions and the quark spin-orbit correlations in the nucleon and should be explored further.

4.3. Higher-twist quark–gluon correlations and power corrections

The twist-3 and twist-4 QCD operators appear in power corrections to polarized and unpolarized DIS structure functions [47, 48]. The instanton effects in these operators depend on the quantum numbers (spin, isospin) and give rise to a hierarchy of structures, which can be compared with experimental data.

The twist-3 and twist-4 operators of dimension 5 with unnatural parity are

$$\mathcal{O}^{\alpha\beta\gamma}(x) = \bar{\psi}(x)\gamma^{\{\alpha}\widetilde{F}^{\beta\}\gamma}(x)\,\tau\psi(x) - \text{traces} \qquad (\text{twist-3})\,, \tag{45}$$

$$\mathcal{O}^{\beta}(x) = \bar{\psi}(x)\gamma_{\alpha}\widetilde{F}^{\beta\alpha}(x)\,\tau\psi(x) \qquad (\text{twist-4})\,, \tag{46}$$

where $\widetilde{F}^{\beta\gamma} = \frac{1}{2}\epsilon^{\beta\gamma\delta\epsilon}F_{\delta\epsilon}$ is the dual field strength and τ is a flavor matrix. The nucleon matrix elements are parametrized as[1]

$$\langle ps|\mathcal{O}^{\alpha\beta\gamma}(0)|ps\rangle \;=\; 2d_2\left(2p^{\{\alpha}p^{\beta\}}s^{\gamma} - 2p^{\{\alpha}s^{\beta\}}p^{\gamma} - \text{traces}\right), \tag{47}$$

$$\langle ps|\mathcal{O}^{\beta}(0)|ps\rangle \;=\; 2f_2 s^{\beta}, \tag{48}$$

where s is the polarization 4-vector, $s^{\mu}p_{\mu} = 0$, $s^2 = -1$. They describe quark–gluon correlations in various spin projections in the polarized nucleon and can be interpreted as electric and magnetic color polarizabilities; see Ref. [49] for a review. d_2 and f_2 appear in the $1/Q^2$ power corrections to the lowest moment of the spin structure function g_1. d_2 also appears in the x^2 moment of g_2, at the same level in $1/Q^2$ as the twist-2 matrix element; the contribution of g_2 to the DIS cross section is overall power-suppressed by $1/Q^2$ [50].

The instanton vacuum makes definite predictions for the spin-dependent higher-twist matrix elements [27]. The twist-3 effective operator obtained from Eq. (45) has hadronic matrix elements of the order of $M^2\bar{\rho}^2 \sim \kappa$, while the twist-4 effective operator obtained from Eq. (46) has matrix element of the order of unity

$$d_2 = \mathcal{O}(\kappa)\,, \qquad f_2 \sim \bar{\rho}^{-2} = \mathcal{O}(1)\,. \tag{49}$$

The reason for the different behavior is the O(4) rotational symmetry of the instanton field. It governs the parametric order of the loop integral appearing in the contraction of the effective operator (see Fig. 6 (a)) and causes a qualitative difference between the results for the twist-3 (= spin-2) and twist-4 (= spin-1) operators.

Numerical predictions for the higher-twist matrix elements from the instanton vacuum have been obtained and can be compared with experimental extractions. The small value of $d_2 \sim$ few $\times\, 10^{-3}$ predicted in Ref. [27] is consistent with the results of g_2 measurements at SLAC and JLab; see Ref. [51] for a global analysis. They are also consistent with modern lattice-QCD calculations using nonperturbative renormalization [52]. The value $f_2^{u-d} \sim 0.2$ GeV^2 predicted in [27] is consistent with the extraction of higher-twist corrections to g_1 in Ref. [53]; for estimates of f_2^{u+d}, see Ref. [54]. While large uncertainties remain, especially in the extraction of f_2 from power corrections, the pattern appears consistent with the instanton predictions.

Other twist-4 operators appear in the power corrections to the unpolarized structure functions. The $1/Q^2$ corrections to F_2 and F_{L} involve quark–gluon and 4-quark operators [48]. The instanton vacuum predicts that one of

[1] The twist-4 matrix element f_2 is defined here with mass dimension (mass)^2, which is natural for the present discussion. In the literature, the mass dimension of f_2 is usually absorbed by factor nucleon mass, $f_2(\text{our}) = m_N^2 f_2(\text{lit})$.

the quark–gluon operators has a large matrix element $\bar{\rho}^{-2} = \mathcal{O}(1)$, while the matrix elements of the 4-quark operators are suppressed [29]. As a consequence, large $1/Q^2$ corrections are predicted in F_{L}, and much smaller corrections in F_2. The pattern is consistent with the results of a phenomenological analysis of higher-twist corrections [29]. The twist-4 operators appearing in the neutrino-structure functions $F_{1\nu}$ and $F_{3\nu}$ have also been computed and have matrix elements $\mathcal{O}(1)$ [27, 55].

In summary, the instanton vacuum allows one to evaluate a range of higher-twist operators governing power corrections to deep-inelastic processes. It predicts a hierarchy of higher-twist matrix elements, with "selection rules" dictated by the O(4) rotational symmetry of the instanton field. Power corrections thus show the footprint of the topological fields in deep-inelastic processes. The approach has been applied to compute matrix elements of chiral-odd higher-twist operators [56] and nonforward matrix elements of higher-twist operators in generalized parton distributions [57]. It can also be extended to compute power corrections in the extraction of quasi-parton distributions [58].

4.4. Trace anomaly and hadron mass decomposition

The twist-4 scalar gluon operator $F^{\mu\nu}F_{\mu\nu}$ appears in the trace anomaly of the EMT and plays an important role in the hadron-mass decomposition in QCD. The instanton vacuum encodes the trace anomaly in the density fluctuations of instantons and allows one to compute and interpret its hadronic matrix elements.

At the classical level, QCD is scale-invariant up to effects proportional to the light-quark masses, and the trace of the EMT is zero, $T^{\mu}{}_{\mu} = 0 + O(m)$. At the quantum level, scale invariance is broken by quantum fluctuations, which require an UV cutoff whose presence is felt even after sending it to infinity (anomaly). The trace of the EMT becomes

$$T^{\mu}{}_{\mu}(x) \;=\; \frac{\beta(g)}{4g^4}F^{\mu\nu}F_{\mu\nu}(x) + m\left[1+\gamma_m(g)\right]\sum_f \bar{\psi}_f\psi_f(x)\,, \tag{50}$$

$$\frac{\beta(g)}{4g^4} \;=\; -\frac{b}{32\pi^2} + \mathcal{O}\left(g^2\right)\,, \qquad \gamma_m(g) = \mathcal{O}\left(g^2\right)\,, \tag{51}$$

where the coefficient b of the beta function is given in Eq. (3), m is the light-quark mass (assumed to be the same for all light flavors here), and γ_m its anomalous dimension. This operator relation equates the trace of the EMT with the dimension-4 gluon operator. It connects the breaking of scale invariance in QCD with the scalar gluon content of hadrons and is fundamental for hadron structure. The expectation value of the EMT in the nucleon state at rest, averaged over the spin, is given by[2]

$$\langle n|T^{\mu}{}_{\mu}(0)|n\rangle = 2m_n^2 \, . \tag{52}$$

This follows from the general form of the nucleon matrix element of the EMT (relativistic covariance, current conservation $\partial_\mu T^{\mu}{}_{\nu} = 0$) and the fact that T^{00} measures the total energy of the state. Equations (50) and (52) imply that

$$\frac{\langle n|F^{\mu\nu}F_{\mu\nu}(0)|n\rangle}{2m_n^2} = -\frac{32\pi^2}{b} + \mathcal{O}(m) \, . \tag{53}$$

This is a remarkable statement: The average of the scalar gluon density in the nucleon state, a quantity arising from nonperturbative dynamics, is constrained by the coefficient of the QCD beta function, a property of perturbation theory. It calls for a mechanical explanation how this connection is realized.

In the instanton vacuum, the trace anomaly is expressed in the fluctuations of the instanton density. The variational approximation to the QCD vacuum is performed with a grand canonical ensemble of instantons, with a variable instanton number $N = N_+ + N_-$ fluctuating with a distribution $P(N)$ (see Fig. 8) [17, 18]. The ensemble average is now understood as

$$\sum_N P(N) \; \langle \ldots \rangle_N \;, \tag{54}$$

where the subscript N denotes the canonical ensemble average used in the derivation of ChSB (see Section 2). The instanton number is proportional to the volume-integrated Euclidean operator $F^2 = F_{\mu\nu}F_{\mu\nu}$,

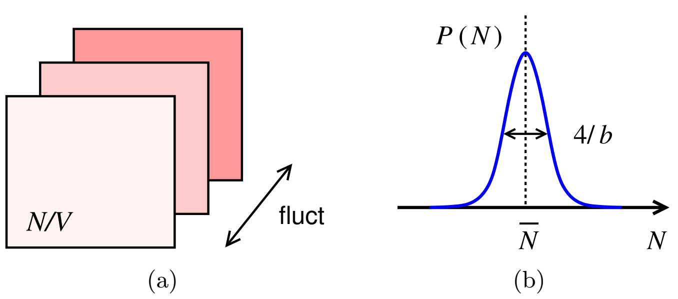

Fig. 8. (a) Instanton density fluctuations in the grand canonical ensemble. (b) Instanton number distribution of Eq. (57).

[2] The nucleon state is denoted here by $|n\rangle$, to avoid confusion with the instanton number N.

$$N = \frac{1}{32\pi^2} \int \mathrm{d}^4 x\, F^2(x)\,, \tag{55}$$

where $32\pi^2$ is the action of a single instanton. The instanton number distribution can be inferred from the low-energy theorems for the vacuum correlation functions of the scalar gluon operator in gluodynamics

$$\left\langle \frac{1}{32\pi^2} \int F^2 \, \frac{1}{32\pi^2} \int F^2 \right\rangle - \left\langle \frac{1}{32\pi^2} \int F^2 \right\rangle^2 = \frac{4}{b} \left\langle \frac{1}{32\pi^2} \int F^2 \right\rangle \tag{56}$$

etc., which are derived by differentiating the renormalized partition function with respect to the inverse coupling constant [59]. It is obtained as [18]

$$P(N) \propto \left(\frac{N}{\bar{N}} \right)^{-bN/4} \mathrm{e}^{bN/4}\,. \tag{57}$$

The variance of the instanton number fluctuations is controlled by the coefficient of the beta function

$$\frac{\overline{(N - \bar{N})^2}}{\bar{N}} = \frac{4}{b}\,, \tag{58}$$

and is known as the topological vacuum compressibility. The instanton number fluctuations are stronger than Poissonian, attesting to the presence of interactions in the system.

Hadronic matrix elements of F^2 are extracted from the 3-point correlation functions of the gluon operator with interpolating operators for the hadronic states. In the connected part of the 3-point correlation function, the contributions proportional to the average instanton number $\bar{N}$ cancel, and the result arises entirely from the fluctuations of N. Schematically,

$$\begin{aligned} \frac{\langle n|F^2(0)|n\rangle}{\langle n|n\rangle} &= \lim_{T\to\infty} \frac{\langle J_n(T) F^2(0) J_n(-T)\rangle_{\mathrm{conn}}}{\langle J_n(T) J_n(-T)\rangle} \\ &= \lim_{T\to\infty} \frac{32\pi^2}{2TV_3} \frac{\overline{(N - \bar{N})^2}}{\bar{N}} \left. \frac{N \dfrac{\mathrm{d}}{\mathrm{d}N} \langle J_n(T) J_n(-T)\rangle_N}{\langle J_n(T) J_n(-T)\rangle_N} \right|_{N=\bar{N}}\,, \end{aligned} \tag{59}$$

where J_n is the nucleon interpolating operator, T is the Euclidean time separation, V_3 is the spatial volume, and $\langle n|n\rangle = 2m_n V_3$ from the normalization of the states [18]. At large times, the 2-point correlation function decays exponentially, with the range given by the nucleon mass. The logarithmic derivative of the correlation function with respect to the instanton number becomes the derivative of nucleon mass

$$\langle J_n(T) J_n(-T) \rangle_N \propto \mathrm{e}^{-2m_n T}, \qquad \frac{1}{2T} \frac{N \dfrac{\mathrm{d}}{\mathrm{d}N} \langle \ldots \rangle_N}{\langle \ldots \rangle_N} = -N \frac{\mathrm{d}m_n}{\mathrm{d}N}. \tag{60}$$

In the instanton vacuum at zero light-quark masses, the only dynamical scale is the instanton density N/V, and hadronic scales arise as powers of this scale according to their naive mass dimension (see Section 2). The nucleon mass thus depends on the instanton density as

$$m_n = [\text{dimensionless constant}] \times \left(\frac{N}{V} \right)^{1/4}. \tag{61}$$

Altogether, Eqs. (59)–(61) determine the nucleon matrix element as

$$\frac{\langle n | F^2(0) | n \rangle}{2m_n^2} = -\frac{32\pi^2}{b}, \tag{62}$$

in agreement with the general result from the trace anomaly of Eq. (53). This remarkable result comes about because in the instanton vacuum the information on the beta function is encoded in the instanton number fluctuations of Eq. (58), and the nucleon mass arises as a power of the instanton density.

The result of Eq. (62) shows several interesting features. *(i)* The expectation value of F^2 in the nucleon state is negative, even though $F^2 > 0$ in the Euclidean metric. This is explained by the fact that the nucleon matrix element measures the change in the vacuum expectation value of F^2 caused by the presence of the nucleon, and the change is negative. *(ii)* In the large-N_c limit, $b \sim N_c$, see Eq. (3). The matrix element of Eq. (62) is, therefore, suppressed in $1/N_c$ compared to its natural size. This circumstance allows for the mixing of gluon and scalar quark/antiquark modes in the t-channel spectral representation of the matrix element and plays an important role in the generalization to nonzero momentum transfer (see Section 4.5).

The trace anomaly of Eq. (50) can also be evaluated in the pion state. In this case, the quark-mass term cannot be neglected, because the pion mass depends on the quark mass as $M_\pi^2 \propto m$. One obtains [42]

$$-\frac{b}{32\pi^2} \frac{\langle \pi | F^2 | \pi \rangle}{2M_\pi} + \frac{\langle \pi | \, m \sum_f \bar{\psi}_f \psi_f | \pi \rangle}{2M_\pi} = M_\pi, \tag{63}$$

where the contribution of $\gamma_m = \mathcal{O}(g^2)$ in the quark-mass term is neglected. It shows that the pion mass arises both from the scalar density of the gluon field (trace anomaly) and the quark mass times the scalar quark density (sigma term). The instanton vacuum allows one to compute both terms separately using the methods described above, and gives [42]

$$-\frac{b}{32\pi^2}\frac{\langle\pi|F^2|\pi\rangle}{2M_\pi} = \frac{M_\pi}{2}\left[1+\mathcal{O}(m)\right] , \tag{64}$$

$$\frac{\langle\pi|\, m\sum_f \bar{\psi}_f\psi_f|\pi\rangle}{2M_\pi} = \frac{M_\pi}{2}\left[1+\mathcal{O}(m)\right] . \tag{65}$$

It shows that the pion mass arises in equal parts from the trace anomaly and the sigma term. Note that the pion matrix element of F^2, Eq. (64), vanishes in the chiral limit, highlighting the interplay of conformal and chiral symmetry breaking. The result for the pion sigma term, Eq. (65), agrees with the result of chiral reduction (soft-pion theorem). Altogether, these results attest to the consistency of the approximations in the description of conformal and chiral symmetry breaking in the instanton vacuum.

In summary, the instanton vacuum describes the hadronic matrix elements of the trace anomaly in accordance with the low-energy theorems of conformal and chiral symmetry breaking. It provides a mechanical picture for the intrusion of the beta function into nonperturbative hadron structure. As such, it represents an essential tool for the study of the hadron mass decomposition and the interplay of conformal and chiral symmetry breaking in QCD.

4.5. Scalar gluon form factors and mechanical properties

Much more information is contained in the form factor of the scalar gluon operator $F^{\mu\nu}F_{\mu\nu}$ at nonzero momentum transfer. The form factors of the EMT define the so-called mechanical properties of hadrons, which have become a field of study in their own right; see Refs. [60, 61] for reviews. The scalar gluon form factor of the nucleon is also measured in heavy quarkonium photo- and electroproduction near threshold; see Ref. [62] and references therein.

The scalar gluon form factors of light hadrons can be computed in the instanton vacuum. An important effect at the nonzero momentum transfer is the mixing of the instanton density fluctuations with the scalar quark–antiquark modes in the effective dynamics arising from ChSB ("glueballs" and "mesons" in colloquial terms). This mixing can be studied within the $1/N_c$ expansion [19, 23, 42]. It is made possible by the fact that the width of the instanton density fluctuations is $b \sim 1/N_c$, so that the action of these modes is of the same order in $1/N_c$ as that of scalar quark–antiquark modes. Practical methods for the computation of nonforward matrix elements of scalar operators have been developed in the regimes of momentum transfers of the order of $Q \sim M$ (soft regime), where the instantons act collectively, and $Q \sim \bar{\rho}^{-1}$ (semi-hard regime), where the scattering process is mediated by single instantons or pairs [23, 63].

Figure 9 shows the results of an instanton vacuum calculation of the gluon scalar form factor of the pion, defined as [see Eq. (50)]

$$G_\pi\left(Q^2\right) = \frac{\langle \pi\left(p'\right) | T^\mu{}_\mu(0)_{\rm glue} | \pi(p) \rangle}{2M_\pi^2} = -\frac{b}{32\pi^2} \frac{\langle \pi\left(p'\right) | F^{\mu\nu} F_{\mu\nu}(0) | \pi(p) \rangle}{2M_\pi^2}, \tag{66}$$

where $Q^2 = -(p'-p)^2$ [42]. This calculation uses the light-front formulation developed in Refs. [40, 41] and subsequent works, and includes instanton pair contributions; see Ref. [42] for details. At the zero momentum transfer, it reproduces the value $G_\pi(0) = 1/2$ obtained from the instanton density fluctuations (see Section 4.4). The instanton vacuum result for the pion scalar gluon form factor agrees well with the recent lattice-QCD calculations [64, 65].

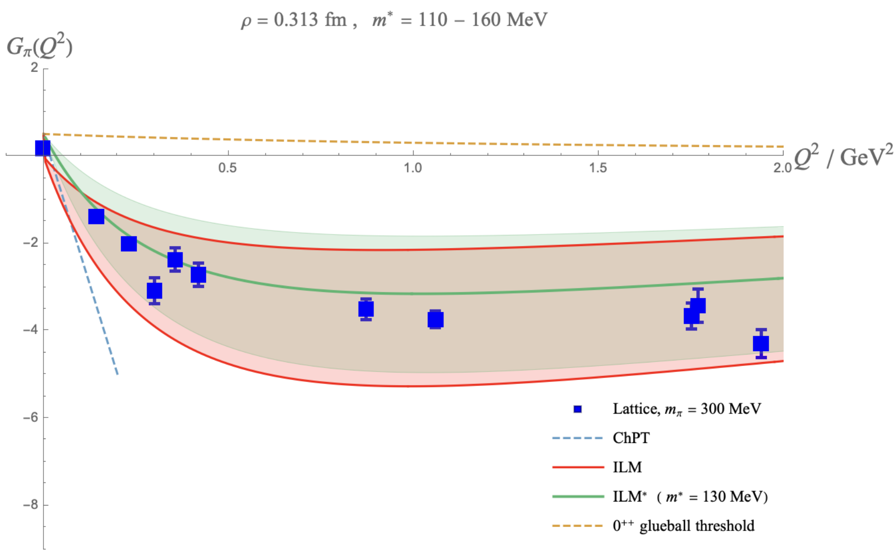

Fig. 9. Pion scalar gluon form factor from the instanton vacuum [42]. Green band: Full instanton vacuum result with uncertainty estimate (see the reference for details). Red bands: Semi-hard contribution $Q \sim 1/\bar{\rho}$ in the instanton vacuum. Blue points: Lattice QCD results [64]. Blue dashed line: Form factor slope from LO chiral perturbation theory. Yellow dashed line: 0^{++} glueball exchange.

In summary, the instanton vacuum predicts the scalar gluon form factors of light hadrons up to momentum transfers $Q \sim$ few GeV^2 based on the non-perturbative gauge field dynamics abstracted from lattice-QCD calculations.

It represents an essential tool in the study of hadron mechanical properties and high-momentum transfer processes. Future studies could *(i)* compute the nucleon and other baryon form factors in the chiral soliton picture in the large-N_c limit, *(ii)* revisit the quark and gluon decomposition of the $\bar{c}$ form factor of Ref. [66] and extend it to the nonzero momentum transfer, *(iii)* compute the amplitude of heavy quarkonium production on light hadrons and other gluonic processes mediated by the instantons.

4.6. Axial anomaly and pseudoscalar gluon form factors

The dimension-4 pseudoscalar gluon operator $F^{\mu\nu}\tilde{F}_{\mu\nu}$ represents the topological charge density of the gauge fields in QCD. The $\mathrm{U(1)_A}$ axial anomaly equates this operator with the divergence of the flavor-singlet axial current, providing a direct connection between the gauge field topology and the spin-flavor dynamics of light quarks. The instanton vacuum encodes the axial anomaly through topological fluctuations of the instanton number, making it possible to compute and interpret the hadronic matrix elements of $F^{\mu\nu}\tilde{F}_{\mu\nu}$. The pseudoscalar meson matrix elements (η' mass *etc.*) have been extensively discussed in the literature [12, 18]; the present review focuses on the nucleon matrix element.

In classical QCD, the axial currents are conserved in the chiral limit. In the quantum theory, the flavor-singlet axial current acquires an anomalous divergence due to quantum fluctuations and renormalization

$$\textstyle\sum_f \partial^\mu \left[\bar{\psi}_f \gamma_\mu \gamma_5 \psi_f\right](x) = \dfrac{N_f}{16\pi^2}\, F^{\mu\nu}\tilde{F}_{\mu\nu}(x) + 2\sum_f m_f \bar{\psi}_f i\gamma_5 \psi_f(x)\,. \tag{67}$$

This operator relation connects the hadronic matrix elements of $F^{\mu\nu}\tilde{F}_{\mu\nu}$ with those of the axial current. The nucleon matrix element of the pseudoscalar gluon operator is parametrized as

$$\langle p'\sigma'|\, F^{\mu\nu}\tilde{F}_{\mu\nu}(0)\,|p\sigma\rangle = A_{\mathrm{P}}\left(q^2\right)\, m_n \bar{u}' i\gamma_5 u\,, \tag{68}$$

where $u \equiv u(p,\sigma)$, $u' \equiv u(p',\sigma')$ are the nucleon 4-spinors and A_{P} is an invariant form factor. Using the axial anomaly of Eq. (67) and the standard representation of the nucleon matrix element of the axial current in terms of the axial and pseudoscalar form factors, and taking the chiral limit, one obtains

$$A_{\mathrm{P}}(0) = 2g_{\mathrm{A}}^{(0)}/N_f\,, \tag{69}$$

where $g_{\mathrm{A}}^{(0)}$ is the nucleon flavor-singlet axial coupling. This remarkable relation connects the nucleon matrix elements of the gluon operator and the light-quark operator of the axial current.

In the instanton vacuum, the axial anomaly is expressed in the fluctuations of the topological charge of the instanton ensemble, *i.e.*, fluctuations of the difference of the number of instantons and antiinstantons

$$\varDelta \equiv N_+ - N_- \, . \tag{70}$$

They can be implemented in the variational approximation with the grand canonical ensemble, in a similar way as the fluctuations of the total instanton number $N = N_+ + N_-$ (see Section 4.4) [17–19]. The fluctuations of $\varDelta$ are described by a distribution $P(\varDelta)$. The instanton number difference is equal to the topological charge in the form of the volume-integrated Euclidean operator $F\tilde{F} \equiv F_{\mu\nu}\tilde{F}_{\mu\nu}$

$$\varDelta = \frac{1}{32\pi^2} \int \mathrm{d}^4 x \; F\tilde{F}(x) \, . \tag{71}$$

The distribution $P(\varDelta)$ can be inferred from the vacuum correlation function of the topological charge,

$$\left\langle \frac{1}{32\pi^2} \int F\tilde{F} \; \frac{1}{32\pi^2} \int F\tilde{F} \right\rangle , \tag{72}$$

the so-called topological susceptibility of the QCD vacuum. The topological susceptibility has been analyzed both in pure gluodynamics and including fermions; it is qualitatively affected by the presence of light fermions and vanishes in the chiral limit [12]. The distribution $P(\varDelta)$ is obtained as [18]

$$P(\varDelta) \propto \exp\left(-\frac{\varDelta^2}{2N} \right) \times \exp\left(\frac{\varDelta^2}{2V \langle \bar{\psi}\psi \rangle} \sum_f^{N_f} m_f^{-1} \right) . \tag{73}$$

The first factor results from gluodynamics (so-called quenched topological susceptibility); the second factor results from the fermion determinant (note that $\langle \bar{\psi}\psi \rangle < 0$). The width of the distribution vanishes when $m_f \to 0$ for at least one flavor f. For quark masses close to the chiral limit, the width of the second factor is much smaller than that of the first, and the width of the overall distribution is dominated by the fermions and their chiral behavior.

The distribution of Eq. (73) can also be derived directly from the fermion determinant in the instanton ensemble with fermions [18]. The instanton ensemble provides a simple explanation of the vanishing of the topological susceptibility in the chiral limit. In the instanton background fields with the nonzero topological charge, $\varDelta \neq 0$ and $N_+ \neq N_-$, the fermion spectrum after

ChSB contains "unbalanced" zero modes, which cause the determinant to vanish in the chiral limit (the functional determinant is the product of the eigenvalues of the modes).

The hadronic matrix elements of $F\tilde{F}$ can be extracted from the 3-point correlation functions, using similar methods as for FF (see Section 4.4). The average is performed with the grand canonical ensemble. The Δ fluctuations connect the gluon operator of Eq. (71) with the effective dynamics of the light quarks, in a way that the $\mathrm{U}(1)_{\mathrm{A}}$ anomaly is realized; see Ref. [18] for details. The chiral singularity of the Δ-fluctuation width is canceled, and a stable result is obtained in the chiral limit. The nucleon matrix element Eq. (68) is obtained consistently with the $\mathrm{U}(1)_{\mathrm{A}}$ anomaly of Eq. (69), with $g_{\mathrm{A}}^{(0)}$ given by the nucleon axial coupling predicted by the effective dynamics of light quarks. The consistent realization of this subtle relation between gluon and light-quark dynamics is a major accomplishment for an effective description of low-energy QCD[3].

The form factors of $F\tilde{F}$ and similar operators at finite momentum transfer can be computed using the methods developed in Refs. [19, 23, 42]. The pseudoscalar form factors at momentum transfers $Q \sim M$ are governed by the mixing of gluon and pseudoscalar quark–antiquark modes, similar to the scalar gluon form factors (see Section 4.5).

In summary, the instanton vacuum describes the hadronic matrix elements of $F\tilde{F}$ in accordance with the $\mathrm{U}(1)_{\mathrm{A}}$ anomaly. It provides a mechanical interpretation of the chiral behavior of the topological susceptibility and illustrates the interplay of chiral dynamics and topological fluctuations in low-energy QCD.

The gluon operators with axial vector quantum numbers appear in the operator expansion of heavy-flavor contributions to the nucleon spin structure functions [67]; their nucleon matrix elements can be evaluated using similar methods as described here.

5. Beyond instantons

The instanton vacuum describes the nonperturbative QCD gauge fields as a superposition of well-separated instantons. The instanton fields are special in that they carry local topological charge ± 1 and induce zero modes of the fermion fields, and thus cause ChSB, which determines the effective dynamics and the structure of light hadrons. This review covers the distinct

[3] The nucleon matrix element Eq. (68) vanishes for zero momentum transfer $q \to 0$ and has to be computed using the position-dependent local operator $F\tilde{F}(x)$. A careful procedure is needed when integrating the position over a finite volume and associating the operator with the topological charge of the ensemble, requiring considerations beyond the treatment of Ref. [18]; see Ref. [28] for a discussion.

gluonic structure induced by well-separated instantons, relevant for the reasons summarized in Section 1. Other vacuum fluctuations can also give rise to strong gauge fields and make significant contributions to the gluonic structure of hadrons.

A broader view of the possible vacuum fluctuations can be obtained from an analysis of the topological landscape of the Yang–Mills gauge theory. Gauge fields configurations are characterized by a winding number N_{CS} (the Chern–Simons number); the energy is a periodic function of N_{CS}, with minima at integer values and a finite potential barrier between them; the height of barrier is determined by the size of the field configurations, ρ [12, 25]. Instantons represent semiclassical tunneling trajectories between minima with $\Delta N_{\mathrm{CS}} = \pm 1$ at zero energy. Recent work [40] has explored the effects of other semiclassical trajectories in the topological landscape: *(i)* instanton–antiinstanton molecules, or streamline paths, where the semiclassical motion does not result in tunneling ("failed tunneling trajectories"). *(ii)* finite-energy tunneling trajectories, or zig–zag paths, where the tunneling process occurs at finite energy and includes both real-time and imaginary-time motion. These types of field configurations are different from well-separated instantons; they do not induce fermion zero modes and thus do not contribute to ChSB. However, they give rise to strong fields and contribute to the Wilson loops [12], high-momentum transfer processes (form factors), and other structures. They should, therefore, be included in the semiclassical description of QCD vacuum.

Including the instanton–antiinstanton molecules in the variational description of instanton vacuum poses several questions [40]. One needs to reassess the instanton density (especially at small sizes $\rho < \bar{\rho}$) and revise the notion of instanton interaction. One also needs to revisit the instanton packing fraction expansion, which provides a simple ordering scheme and guarantees conservation laws (current conservation, energy-momentum conservation). The benefit of including instanton–antiinstanton molecules is that one obtains quantitative estimates for the many structures that are absent in the dilute instanton medium, especially the twist-2 gluon density.

Including the effects of instanton–antiinstanton molecules in the effective dynamics arising from ChSB ($1/N_c$ expansion, chiral soliton picture of nucleon) and in the effective operator approach presents many opportunities for further development. It can lead to a more realistic semiclassical description of light hadron structure, especially gluonic structure [23].

6. Related subjects

This review focuses on the gluonic properties of light hadrons, whose structure is essentially determined by ChSB. The instanton vacuum can also be employed to study heavy–light hadrons [68–70], where ChSB controls the dynamics of the light flavors in the presence of the heavy quark. The instanton vacuum and its extensions can also be applied to study heavy quarkonia [71–76]; in these systems, semiclassical trajectories beyond well-separated instantons are expected to play an important role.

The effective operator method can also be used to compute vacuum expectation values of higher-dimensional QCD quark–gluon operators, such as the dimension-5 chiral-odd operator $\bar{\psi}(x)(\lambda^a/2)\sigma^{\mu\nu}\psi(x)F^a_{\mu\nu}(x)$ [of the form of Eq. (23)] and similar dimension-7 operators [77, 78]. These higher-dimensional vacuum condensates are generalizations of the chiral order parameter and sensitive to the gluon fields active in ChSB. Comparison of the instanton vacuum results with lattice-QCD calculations provides direct information on the instanton-size distribution in the vacuum, complementary to cooling studies.

This material is based upon work supported by the U.S. Department of Energy, Office of Science, Office of Nuclear Physics under contract DE-AC05-06OR23177. The research reported here takes place in the context of the Topical Collaboration "3D quark–gluon structure of hadrons: mass, spin, tomography" (Quark–Gluon Tomography Collaboration) supported by the U.S. Department of Energy, Office of Science, Office of Nuclear Physics under contract DE-SC0023646.

REFERENCES

[1] C.G. Callan, Jr., R.F. Dashen, D.J. Gross, «The structure of the gauge theory vacuum», *Phys. Lett. B* **63**, 334 (1976).

[2] C.G. Callan, Jr., R.F. Dashen, D.J. Gross, «Toward a theory of the strong interactions», *Phys. Rev. D* **17**, 2717 (1978).

[3] A.I. Vainshtein, V.I. Zakharov, V.A. Novikov, M.A. Shifman, «ABC's of instantons», *Sov. Phys. Usp.* **25**, 195 (1982).

[4] T. Banks, A. Casher, «Chiral symmetry breaking in confining theories», *Nucl. Phys. B* **169**, 103 (1980).

[5] D.B. Leinweber, «Visualizations of the QCD vacuum», in: «Proceedings of Workshop on Light-Cone QCD and Nonperturbative Hadron Physics», Adelaide, Australia, 13–22 December, 1999, pp. 138–143, arXiv:hep-lat/0004025.

[6] C. Bonati, M. D'Elia, «Comparison of the gradient flow with cooling in SU(3) pure gauge theory», *Phys. Rev. D* **89**, 105005 (2014), arXiv:1401.2441 [hep-lat].

[7] C. Alexandrou *et al.*, «Comparison of topological charge definitions in Lattice QCD», *Eur. Phys. J. C* **80**, 424 (2020), arXiv:1708.00696 [hep-lat].

[8] A. Athenodorou *et al.*, «Instanton liquid properties from lattice QCD», *J. High Energy Phys.* **2018**, 140 (2018), arXiv:1801.10155 [hep-lat].

[9] E.V. Shuryak, «The role of instantons in quantum chromodynamics. (I). Physical vacuum», *Nucl. Phys. B* **203**, 93 (1982).

[10] D. Diakonov, V.Y. Petrov, «Instanton based vacuum from Feynman variational principle», *Nucl. Phys. B* **245**, 259 (1984).

[11] D. Diakonov, «Instantons at work», *Prog. Part. Nucl. Phys.* **51**, 173 (2003), arXiv:hep-ph/0212026.

[12] T. Schäfer, E.V. Shuryak, «Instantons in QCD», *Rev. Mod. Phys.* **70**, 323 (1998), arXiv:hep-ph/9610451.

[13] E.V. Shuryak, «The role of instantons in quantum chromodynamics. (II). Hadronic structure», *Nucl. Phys. B* **203**, 116 (1982).

[14] D. Diakonov, V.Y. Petrov, «A theory of light quarks in the instanton vacuum», *Nucl. Phys. B* **272**, 457 (1986).

[15] D. Diakonov, V.Y. Petrov, «Spontaneous breaking of chiral symmetry in the instanton vacuum», in: G.M. Zinovev, V.P. Shelest (Eds.) «Hadron Matter under Extreme Conditions», *Naukova Dumka*, Kiev 1986, p. 192. Published in Russian.

[16] P.V. Pobylitsa, «The quark propagator and correlation functions in the instanton vacuum», *Phys. Lett. B* **226**, 387 (1989).

[17] M.A. Nowak, J.J.M. Verbaarschot, I. Zahed, «Instantons and chiral dynamics», *Phys. Lett. B* **228**, 251 (1989).

[18] D. Diakonov, M.V. Polyakov, C. Weiss, «Hadronic matrix elements of gluon operators in the instanton vacuum», *Nucl. Phys. B* **461**, 539 (1996), arXiv:hep-ph/9510232.

[19] M. Kacir, M. Prakash, I. Zahed, «Hadrons and QCD Instantons: A Bosonized View», *Acta Phys. Pol. B* **30**, 287 (1999), arXiv:hep-ph/9602314.

[20] D. Diakonov, V.Y. Petrov, P.V. Pobylitsa, «A chiral theory of nucleons», *Nucl. Phys. B* **306**, 809 (1988).

[21] E. Witten, «Baryons in the $1/N$ expansion», *Nucl. Phys. B* **160**, 57 (1979).

[22] C.V. Christov *et al.*, «Baryons as non-topological chiral solitons», *Prog. Part. Nucl. Phys.* **37**, 91 (1996), arXiv:hep-ph/9604441.

[23] W.-Y. Liu, E. Shuryak, I. Zahed, «Glue in hadrons at medium resolution and the QCD instanton vacuum», *Phys. Rev. D* **110**, 054005 (2024), arXiv:2404.03047 [hep-ph].

[24] G. 't Hooft, «Computation of the quantum effects due to a four-dimensional pseudoparticle», *Phys. Rev. D* **14**, 3432 (1976); *Erratum ibid.* **18**, 2199 (1978).

[25] D. Diakonov, «Topology and confinement», *Nucl. Phys. B Proc. Suppl.* **195**, 5 (2009), arXiv:0906.2456 [hep-ph].

[26] D. Diakonov, M.I. Eides, «Chiral lagrangian from a functional integral over quarks», *JETP Lett.* **38**, 433 (1983).

[27] J. Balla, M.V. Polyakov, C. Weiss, «Nucleon matrix elements of higher twist operators from the instanton vacuum», *Nucl. Phys. B* **510**, 327 (1998), arXiv:hep-ph/9707515.

[28] C. Weiss, «Nucleon matrix element of Weinberg's CP-odd gluon operator from the instanton vacuum», *Phys. Lett. B* **819**, 136447 (2021), arXiv:2103.13471 [hep-ph].

[29] B. Dressler, M. Maul, C. Weiss, «Twist four contribution to unpolarized structure functions F_L and F_2 from instantons», *Nucl. Phys. B* **578**, 293 (2000), arXiv:hep-ph/9906444.

[30] W.-Y. Liu, «Generic framework for non-perturbative QCD in light hadrons», arXiv:2501.07776 [hep-ph].

[31] J.-Y. Kim, C. Weiss, «Instanton effects in twist-3 generalized parton distributions», *Phys. Lett. B* **848**, 138387 (2024), arXiv:2310.16890 [hep-ph].

[32] D. Diakonov *et al.*, «Nucleon parton distributions at low normalization point in the large N_c limit», *Nucl. Phys. B* **480**, 341 (1996), arXiv:hep-ph/9606314.

[33] D. Diakonov *et al.*, «Unpolarized and polarized quark distributions in the large N_c limit», *Phys. Rev. D* **56**, 4069 (1997), arXiv:hep-ph/9703420.

[34] STAR Collaboration (L. Adamczyk *et al.*), «Measurement of Longitudinal Spin Asymmetries for Weak Boson Production in Polarized Proton–Proton Collisions at RHIC», *Phys. Rev. Lett.* **113**, 072301 (2014), arXiv:1404.6880 [nucl-ex].

[35] STAR Collaboration (J. Adam *et al.*), «Measurement of the longitudinal spin asymmetries for weak boson production in proton–proton collisions at $\sqrt{s} = 510$ GeV», *Phys. Rev. D* **99**, 051102 (2019), arXiv:1812.04817 [hep-ex].

[36] PHENIX Collaboration (A. Adare *et al.*), «Measurement of parity-violating spin asymmetries in $W^{\pm}$ production at midrapidity in longitudinally polarized $p + p$ collisions», *Phys. Rev. D* **93**, 051103 (2016), arXiv:1504.07451 [hep-ex].

[37] PHENIX Collaboration (A. Adare *et al.*), «Cross section and longitudinal single-spin asymmetry A_L for forward $W^{\pm} \to \mu^{\pm}\nu$ production in polarized $p + p$ collisions at $\sqrt{s} = 510$ GeV», *Phys. Rev. D* **98**, 032007 (2018), arXiv:1804.04181 [hep-ex].

[38] C. Cocuzza, W. Melnitchouk, A. Metz, N. Sato, «Polarized antimatter in the proton from a global QCD analysis», *Phys. Rev. D* **106**, L031502 (2022), arXiv:2202.03372 [hep-ph].

[39] R.G. Edwards *et al.*, «Non-singlet quark helicity PDFs of the nucleon from pseudo-distributions», *J. High Energy Phys.* **2023**, 086 (2023), arXiv:2211.04434 [hep-lat].

[40] E. Shuryak, I. Zahed, «Hadronic structure on the light front. I. Instanton effects and quark–antiquark effective potentials», *Phys. Rev. D* **107**, 034023 (2023), arXiv:2110.15927 [hep-ph].

[41] E. Shuryak, I. Zahed, «Hadronic structure on the light front. II. QCD strings, Wilson lines, and potentials», *Phys. Rev. D* **107**, 034024 (2023), arXiv:2111.01775 [hep-ph].

[42] W.-Y. Liu, E. Shuryak, C. Weiss, I. Zahed, «Pion gravitational form factors in the QCD instanton vacuum. I», *Phys. Rev. D* **110**, 054021 (2024), arXiv:2405.14026 [hep-ph].

[43] M. Glück, E. Reya, A. Vogt, «Dynamical parton distributions revisited», *Eur. Phys. J. C* **5**, 461 (1998), arXiv:hep-ph/9806404.

[44] C. Lorcé, L. Mantovani, B. Pasquini, «Spatial distribution of angular momentum inside the nucleon», *Phys. Lett. B* **776**, 38 (2018), arXiv:1704.08557 [hep-ph].

[45] C. Lorcé, «Spin-orbit correlations in the nucleon», *Phys. Lett. B* **735**, 344 (2014), arXiv:1401.7784 [hep-ph].

[46] J.-Y. Kim, H.-Y. Won, H.-C. Kim, C. Weiss, «Spin-orbit correlations in the nucleon in the large-N_c limit», *Phys. Rev. D* **110**, 054026 (2024), arXiv:2403.07186 [hep-ph].

[47] E.V. Shuryak, A.I. Vainshtein, «Theory of power corrections to deep inelastic scattering in quantum chromodynamics. (II). Q^{-4} effects: polarized target», *Nucl. Phys. B* **201**, 141 (1982).

[48] E.V. Shuryak, A.I. Vainshtein, «Theory of power corrections to deep inelastic scattering in quantum chromodynamics. (I). Q^{-2} effects», *Nucl. Phys. B* **199**, 451 (1982).

[49] S.E. Kuhn, J.P. Chen, E. Leader, «Spin structure of the nucleon — status and recent results», *Prog. Part. Nucl. Phys.* **63**, 1 (2009), arXiv:0812.3535 [hep-ph].

[50] B. Ehrnsperger, A. Schafer, L. Mankiewicz, «OPE analysis for polarized deep inelastic scattering», *Phys. Lett. B* **323**, 439 (1994), arXiv:hep-ph/9311285.

[51] N. Sato *et al.*, «Iterative Monte Carlo analysis of spin-dependent parton distributions», *Phys. Rev. D* **93**, 074005 (2016), arXiv:1601.07782 [hep-ph].

[52] M. Gockeler *et al.*, «Investigation of the second moment of the nucleon's g_1 and g_2 structure functions in two-flavor lattice QCD», *Phys. Rev. D* **72**, 054507 (2005), arXiv:hep-lat/0506017.

[53] A.V. Sidorov, C. Weiss, «Higher twists in polarized DIS and the size of the constituent quark», *Phys. Rev. D* **73**, 074016 (2006), arXiv:hep-ph/0602142.

[54] N.-Y. Lee, K. Goeke, C. Weiss, «Spin dependent twist four matrix elements from the instanton vacuum: Flavor singlet and nonsinglet», *Phys. Rev. D* **65**, 054008 (2002), arXiv:hep-ph/0105173.

[55] C. Weiss, «Modeling power corrections to the Bjorken sum rule for the neutrino structure function F_1», *J. Phys. G: Nucl. Part. Phys.* **29**, 1981 (2003), arXiv:hep-ph/0210132.

[56] B. Dressler, M.V. Polyakov, «On the twist-three contribution to h_L in the instanton vacuum», *Phys. Rev. D* **61**, 097501 (2000), arXiv:hep-ph/9912376.

[57] D.V. Kiptily, M.V. Polyakov, «Genuine twist three contributions to the generalized parton distributions from instantons», *Eur. Phys. J. C* **37**, 105 (2004), arXiv:hep-ph/0212372.

[58] Y. Liu, I. Zahed, «Small size instanton contributions to the quark quasi-PDF and matching kernel», arXiv:2102.07248 [hep-ph].

[59] V.A. Novikov, M.A. Shifman, A.I. Vainshtein, V.I. Zakharov, «Are all hadrons alike?», *Nucl. Phys. B* **191**, 301 (1981).

[60] C. Lorcé, H. Moutarde, A.P. Trawiński, «Revisiting the mechanical properties of the nucleon», *Eur. Phys. J. C* **79**, 89 (2019), arXiv:1810.09837 [hep-ph].

[61] M.V. Polyakov, P. Schweitzer, «Forces inside hadrons: pressure, surface tension, mechanical radius, and all that», *Int. J. Mod. Phys. A* **33**, 1830025 (2018), arXiv:1805.06596 [hep-ph].

[62] B. Duran *et al.*, «Determining the gluonic gravitational form factors of the proton», *Nature* **615**, 813 (2023), arXiv:2207.05212 [nucl-ex].

[63] W.-Y. Liu, E. Shuryak, I. Zahed, «Pion gravitational form factors in the QCD instanton vacuum. II», *Phys. Rev. D* **110**, 054022 (2024), arXiv:2405.16269 [hep-ph].

[64] B. Wang *et al.*, «Trace anomaly form factors from lattice QCD», *Phys. Rev. D* **109**, 094504 (2024), arXiv:2401.05496 [hep-lat].

[65] D.C. Hackett, P.R. Oare, D.A. Pefkou, P.E. Shanahan, «Gravitational form factors of the pion from lattice QCD», *Phys. Rev. D* **108**, 114504 (2023), arXiv:2307.11707 [hep-lat].

[66] M.V. Polyakov, H.-D. Son, «Nucleon gravitational form factors from instantons: forces between quark and gluon subsystems», *J. High Energy Phys.* **2018**, 156 (2018), arXiv:1808.00155 [hep-ph].

[67] M. Franz, M.V. Polyakov, K. Goeke, «Heavy quark mass expansion and intrinsic charm in light hadrons», *Phys. Rev. D* **62**, 074024 (2000), arXiv:hep-ph/0002240.

[68] S. Chernyshev, M.A. Nowak, I. Zahed, «Heavy mesons in a random instanton gas», *Phys. Lett. B* **350**, 238 (1995), arXiv:hep-ph/9409207.

[69] S. Chernyshev, M.A. Nowak, I. Zahed, «Heavy hadrons and QCD instantons», *Phys. Rev. D* **53**, 5176 (1996), arXiv:hep-ph/9510326.

[70] K.-H. Hong, H.-C. Kim, M.M. Musakhanov, N. Rakhimov, «Heavy–light quark systems from the QCD instanton vacuum: $N_f = 1$ light flavor case», *Phys. Rev. D* **110**, 114044 (2024), arXiv:2410.13279 [hep-ph].

[71] D. Diakonov, V.Y. Petrov, P.V. Pobylitsa, «The Wilson loop and heavy quark potential in the instanton vacuum», *Phys. Lett. B* **226**, 372 (1989).

[72] U.T. Yakhshiev *et al.*, «Instanton effects on the heavy-quark static potential», *Chinese Phys. C* **41**, 083102 (2017), arXiv:1602.06074 [hep-ph].

[73] M. Musakhanov, N. Rakhimov, U.T. Yakhshiev, «Heavy quark correlators in an instanton liquid model with perturbative corrections», *Phys. Rev. D* **102**, 076022 (2020), arXiv:2006.01545 [hep-ph].

[74] E. Shuryak, I. Zahed, «Hadronic structure on the light front. III. The Hamiltonian, heavy quarkonia, spin, and orbit mixing», *Phys. Rev. D* **107**, 034025 (2023), arXiv:2112.15586 [hep-ph].

[75] N. Miesch, E. Shuryak, I. Zahed, «Baryons and tetraquarks using instanton-induced interactions», *Phys. Rev. D* **109**, 014022 (2024), arXiv:2308.05638 [hep-ph].

[76] N. Miesch, E. Shuryak, I. Zahed, «Bridging hadronic and vacuum structure by heavy quarkonia», *Phys. Rev. D* **111**, 034006 (2025), arXiv:2403.18700 [hep-ph].

[77] M.V. Polyakov, C. Weiss, «Mixed quark–gluon condensate from instantons», *Phys. Lett. B* **387**, 841 (1996), arXiv:hep-ph/9607244.

[78] M.V. Polyakov, C. Weiss, «Estimates of higher dimensional vacuum condensates from the instanton vacuum», *Phys. Rev. D* **57**, 4471 (1998), arXiv:hep-ph/9710534.